
RMT-BVQA: Recurrent Memory Transformer-based Blind Video Quality Assessment for Enhanced Video Content

Tianhao Peng^{†‡}, Chen Feng^{†‡}, Duolikun Danier[†], Fan Zhang[†], David Bull[†]

[†] Visual Information Lab, University of Bristol, BS1 5DD, United Kingdom
{ha21615, chen.feng, duolikun.danier, fan.zhang, dave.bull}@bristol.ac.uk

Abstract

With recent advances in deep learning, numerous algorithms have been developed to enhance video quality, reduce visual artefacts and improve perceptual quality. However, little research has been reported on the quality assessment of enhanced content - the evaluation of enhancement methods is often based on quality metrics that were designed for compression applications. In this paper, we propose a novel blind deep video quality assessment (VQA) method specifically for enhanced video content. It employs a new Recurrent Memory Transformer (RMT) based network architecture to obtain video quality representations, which is optimised through a novel content-quality-aware contrastive learning strategy based on a new database containing 13K training patches with enhanced content. The extracted quality representations are then combined through linear regression to generate video-level quality indices. The proposed method, RMT-BVQA, has been evaluated on the VDPVE (VQA Dataset for Perceptual Video Enhancement) database through a five-fold cross validation. The results show its superior correlation performance when compared to ten existing no-reference quality metrics.

1 Introduction

Video content is now everywhere! It is by far the largest global Internet bandwidth consumer, with a wide range of applications including consumer video, video conferencing, and gaming. It has been reported that in 2022, each individual in the United Kingdom spent 4.5 hours per day (on average) consuming video content on different platforms [43]. Due to various conditions associated with video capture, editing, and delivery, streamed content often contains a range of visual artefacts, which can affect the quality of a user's experience. To address this issue, enhancement approaches have been developed, with the aim of reducing visible artefacts and improving overall perceptual quality, e.g. colour transform [16, 34], deblurring [60, 25], deshaking [15], post processing [12, 57], super resolution [9, 56], etc. In particular, more recently, driven by the advances of deep generative models [36, 10, 6], we have seen more effective methods proposed that offer promising enhancement results.

In order to evaluate the performance of these methods, enhanced content can be assessed subjectively through psychophysical experiments or objectively using various video quality metrics. While the former offers ground-truth results, objective video quality assessment (VQA) methods are used more often in practice due to their higher efficiency and lower cost [3]. In the video enhancement literature, blind (without pristine reference sources) quality metrics are more relevant compared to full- and reduced- reference VQA methods. This is because, in most cases, the enhancement operation is performed at the user end, where the reference content is unavailable.

Preprint.

[‡] Equal contribution.

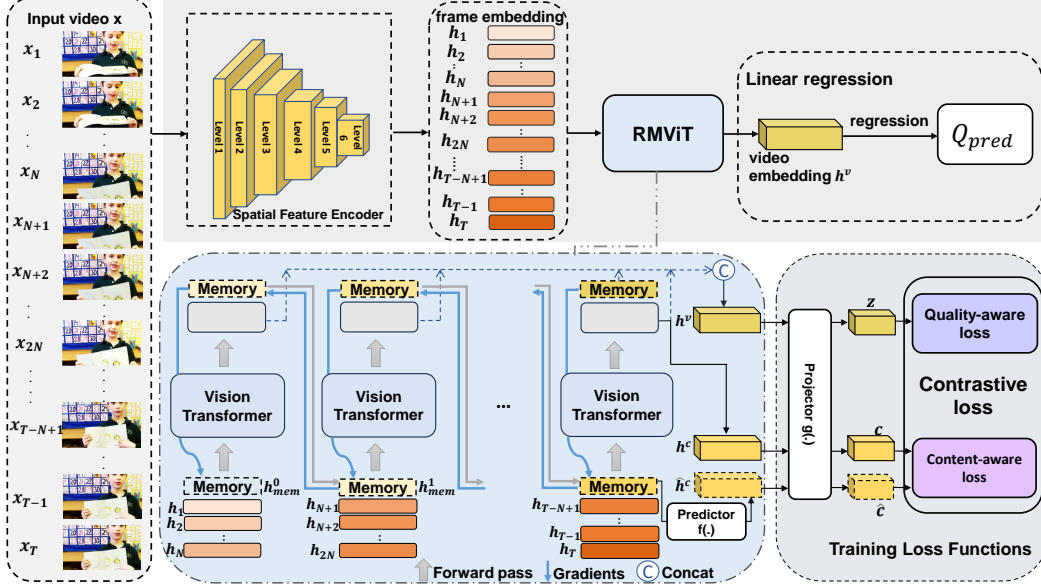


Figure 1: Illustration of the proposed RMT-BVQA framework.

Conventional blind VQA methods [39, 41, 50] are predominantly based on various features extracted in the spatio-temporal or/and frequency domains. Recent advances in this research area favour deep learning-based models employing convolutional neural networks (CNNs) [1, 30] or Vision Transformers (ViTs) [52]. However, these methods tend to exhibit inconsistent performance due to the lack of large and diverse training databases (in particular, for enhanced video content) and inefficient training methodologies. Furthermore, in order to make use of the limited ground-truth quality labels in existing datasets, end-to-end training at the video level is required, but infeasible due to the computation constraints (e.g. memory) with most existing hardware. As a result, many methods [52, 55] resort to sub-sampling videos before evaluating their quality, leading to a significant loss of information. Moreover, it is also noted that most of these blind VQA models were originally optimised and validated on compressed videos that contain artefact types and (spatio-temporal) distributions that differ compared to enhanced content. This can lead to inconsistent metric performance when used to assess enhancement video content.

Inspired by recent works in contrastive learning [37, 59] and the recurrent memory mechanism [2], this paper proposes a blind VQA method, RMT-BVQA (illustrated in Figure 1), based on a new content-quality-aware self-supervised learning methodology and a novel Recurrent Memory Vision Transformer (RMViT) module. This approach first generates a comprehensive representation of the video through dynamically processing global and local information across video frames using the proposed RMViT module. The video representation is then used to predict the final sequence quality index through linear regression. To facilitate the optimisation of the RMViT module through contrastive learning, we have also created a large-scale database containing content generated by various enhancement methods. The primary contributions of this work are summarised as follows.

- **Recurrent Memory Vision Transformer (RMViT) module:** To characterise the artefacts exhibiting in the enhanced video content, we designed a new network architecture based on the recurrent memory mechanism [2], which has been employed in language modelling [2], for capturing both short-term temporal dynamics and long-term global information. This also aligns well with the visual persistence characteristic of the human visual system [8]. Moreover, this facilitates end-to-end training at the video level, without sub-sampling the video content, and the recurrence nature allows our model to evaluate videos of variable length. This is the **first** time when the recurrent memory mechanism is used for the video quality assessment task.
- **Content-quality-aware self-supervised learning:** We developed a new self-supervised learning strategy based on a content-quality-aware loss function. This training methodology enables us to optimise the proposed RMViT module based on a large amount of training material without performing expensive and time consuming subjective tests. Here we, for the first time, used a

proxy perceptual quality metric to support the quality-aware contrastive learning, inspired by the ranking-based training strategies proposed in [13, 45].

- **A new training dataset:** We developed a large and diverse training dataset containing various types of enhanced video content to support the proposed content-quality-aware contrastive learning strategy.

The proposed method has been evaluated on the VQA Dataset for Perceptual Video Enhancement (VDPVE) [14] and achieves superior performance over ten existing no-reference VQA methods based on a five-fold cross validation experiment, with an average Spearman Ranking Order Correlation Coefficient (SRCC) of 0.8209.

2 Related Work

Objective quality assessment is one of the most important research topics in the field of image processing. It aims to accurately predict the perceptual quality of an input signal given (full reference) or without (no reference) the corresponding reference content. Objective quality metrics play an essential role in comparing different image/video processing methods and supporting algorithm optimisation, e.g. in the rate quality optimisation for compression [42] or as loss functions for learning-based approaches [36]. In the context of video enhancement, since the quality assessment of enhanced content is typically performed when the original reference video is absent, we primarily focus on the no-reference scenario here.

Conventional no-reference quality assessment methods often employ hand-crafted models to observe the input content through spatial, temporal and/or frequency feature extraction. For example, V-BLIINDS [46] employs a spatio-temporal natural scene statistics (NSS) model to quantify motion coherency in video scenes; TLVQM [24] calculates features at various scales from a selection of representative video frames; VIDEVAL [50] predicts video quality by extracting various spatio-temporal artefact features such as motion, jerkiness and blurriness. Other notable contributions include NIQE [41], BRISQUE [39] and V-CORNIA [54]. A more comprehensive review on blind image and video quality metrics can be found in [47].

Learning-based no-reference quality assessment has become more popular recently, inspired by advances in machine learning. Early attempts [23] use various regression models to fit and predict quality indices based on extracted features and conventional quality metrics. More recently, deep neural networks have been utilised for both feature extraction and quality regression to offer improved prediction performance, with important examples including VSFA [30], BVQA [29], SimpleVQA [26], FAST-VQA [52], TB-VQA [53] and SB-VQA [20].

Training methodology. For deep learning-based quality models, it is key to have a large, diverse and representative training database. However, creating such databases is costly since groundtruth quality labels are typically annotated through subjective tests involving human participants. To address this issue, Feng et al. [13] used proxy quality metrics for training content labelling and developed a ranking-inspired training strategy to maintain the reliability of the quality annotation. Moreover, self-supervised learning methods have also been employed which convert the quality labelling into an auxiliary task [37, 38, 59].

Quality assessment for enhanced video content is an underexplored research topic. Previous works typically fine-tune existing blind quality models using enhanced content. A grand challenge [32] was organised in 2023 specifically for enhanced video quality assessment, based on a public training database (VDPVE) [14] which contains enhanced video sequences generated through contrast enhancement, deshaking and deblurring.

3 Proposed Method

The proposed RMT-BVQA framework is illustrated in Figure 1. It first takes each frame of the input video and transforms it into a one-dimensional embedding using a Spatial Feature Encoder. The extracted embeddings are then sequentially processed by the RMViT (Recurrent Memory Vision Transformer) module to generate the representation of the input video. Finally, a linear ridge regression is employed to output the final sequence quality index. The network architectures employed

for each module in this framework, the training database, and the model optimisation strategy are described below in detail.

3.1 Network architecture

Spatial Feature Encoder. Here we employ a pre-trained ResNet-50 based [18] network which was optimised in a deep image quality model [37] for spatial feature extraction. The network parameters are fixed during our training process for the proposed RMT-BVQA. For each frame, a 2048×1 embedding is extracted.

RMViT module. Considering that artefact types and distributions in the enhanced video content are different from those in compressed content (on which most blind VQA methods are optimised and validated), we designed a new Recurrent Memory Vision Transformer (RMViT) module to effectively capture both the local temporal dynamic and global information within the input video sequence. This is inspired by the recurrent memory mechanism [2] that has been successfully integrated into language models. This mechanism can process and “remember” both local and global information and pass the “memory” between segments within a long sequence using the recurrence structure [2], thus is applicable to videos of any length. As far as we know, this is the first time when the recurrent memory mechanism is applied for the quality assessment task.

As shown in Figure 1, in the first recurrent iteration, the proposed RMViT module takes N frame embeddings ($\mathbf{h}_1 \mathbf{h}_2 \dots \mathbf{h}_N$, corresponding to the first segment in the video) extracted by the Spatial Feature Encoder together with empty memory ($\mathbf{h}_{\text{mem}}^0 \in \mathbb{R}^{2048 \times M}$) as input, where N is a configurable hyperparameter that defines the length of each video segment and M denotes the number of the memory tokens. Specifically, for the first iteration, the input of RMViT is given below:

$$\mathbf{H}_0 = [\mathbf{h}_{\text{mem}}^0 \circ \mathbf{h}_1 \circ \mathbf{h}_2 \circ \dots \circ \mathbf{h}_N], \quad (1)$$

in which \circ stands for the concatenation operation. \mathbf{H}_0 will then be processed by a Vision Transformer with the output, $\tilde{\mathbf{H}}_0 \in \mathbb{R}^{2048 \times (M+N)}$:

$$\tilde{\mathbf{H}}_0 := [\mathbf{h}_{\text{mem}}^1 \circ \tilde{\mathbf{h}}_1 \circ \tilde{\mathbf{h}}_2 \circ \dots \circ \tilde{\mathbf{h}}_N] = \text{ViT}(\mathbf{H}_0) \quad (2)$$

For the second recurrent iteration, we further combine the frame embeddings of the next video segment ($\mathbf{h}_{N+1} \mathbf{h}_{N+2} \dots \mathbf{h}_{2N}$) with the memory token $\mathbf{h}_{\text{mem}}^1$ in $\tilde{\mathbf{H}}_0$ as the input of the Vision Transform \mathbf{H}_1 to obtain $\tilde{\mathbf{H}}_1$.

$$\mathbf{H}_1 = [\mathbf{h}_{\text{mem}}^1 \circ \mathbf{h}_{N+1} \circ \mathbf{h}_{N+2} \circ \dots \circ \mathbf{h}_{2N}], \text{ and} \quad (3)$$

$$\tilde{\mathbf{H}}_1 := [\mathbf{h}_{\text{mem}}^2 \circ \tilde{\mathbf{h}}_{N+1} \circ \tilde{\mathbf{h}}_{N+2} \circ \dots \circ \tilde{\mathbf{h}}_{2N}] = \text{ViT}(\mathbf{H}_1). \quad (4)$$

After processing all segments in the input video, the RMViT finally outputs a video-level embedding $\mathbf{h}^v \in \mathbb{R}^{2048 \times 1}$ by performing average pooling on the concatenation of the memory tokens generated in the last recurrent iteration and all the Vision Transformer processed frame embeddings, $[\mathbf{h}_{\text{mem}}^S \circ \tilde{\mathbf{h}}_1 \circ \tilde{\mathbf{h}}_2 \circ \dots \circ \tilde{\mathbf{h}}_T]$. It is noted that this is slightly different to the original recurrent memory mechanism [2], where only the memory in the last iteration contributes to the module output. This modification helps to capture the temporal dynamics across the entire video sequence and enhances the stability of the model. Here S stands for the number of segments, while T represents the total number of frames in S segments. In cases when the last segment contains frames fewer than N , this segment will be discarded.

Regression. The final output of the RMViT module, \mathbf{h}^v , is passed to a linear ridge regressor (the same as in [38]) in order to obtain the sequence level quality index, Q_{pred} . Here the regressor is optimised during the cross validation experiment, in which the model parameters of the RMViT are fixed.

3.2 Training Database Generation

To support the training of the RMViT module, we have collected 149 source videos (with a spatial resolution of 1080p or 720p) from five publicly available datasets including BVI-DVC [35], KoNViD-1k [19], LIVE-VQC [48], Live-Qualcomm [17], and YouTube-UGC [51]. Three primary visual artefacts¹ (as defined in VDPVE [14]) including (i) colour / brightness / contrast degradation,

¹The investigation of other types of enhanced content was not the focus of this work, but remains as future work.

(ii) camera shaking and (iii) blurring, are synthesised (for (iii), through Gaussian filtering) or inherent within the source content (for (i) and (ii)). These videos are then processed using 12 different conventional and learning-based enhancement methods to generate a total of 596 enhanced video sequences. The detailed database generation process is summarised in Table 1.

Class	Number of Source Videos	Enhancement Methods
Colour, Brightness and Contrast Enhancement	44	ACE [16], DCC-Net [58], MBLLEN [34], CapCut [49]
Deshaking	50	GlobalFlowNet [15], Adobe Premiere Pro [44], CapCut (minimum cropping mode) [49], CapCut (most stable mode) [49]
Deblurring	55	ESTRNN [60], DeblurGANv2 [25], BasicVSR++ [4], Adobe Premiere Pro [44]

Table 1: Training database generation.

Each enhanced video and its corresponding reference counterpart are then randomly segmented with a non-overlapping spatio-temporal sliding window to produce training patches with the size of 256 (height) $\times 256$ (width) $\times 3$ (channel) $\times 72$ (temporal length). The reference patches here are only used to generate pseudo-labels for quality classification and are not input into the model. This results in 13,156 (enhanced and reference) patch pairs.

3.3 Training Strategy

In self-supervised learning, when the model is difficult to optimise directly for its primary task, it is often trained to perform a related pretext task, which can be learnt more effectively. In our case, since assessing the quality of enhanced video content is a challenging task and the corresponding labels are difficult to obtain, inspired by contrastive learning [21, 27], we employ a projector network (with two layers of multilayer perceptron), $g(\cdot)$, to transform the original task into two classification problems focusing on content and quality classification, rather than predicting absolute quality indices.

Specifically, the projector first takes the output of the RMViT, \mathbf{h}^v , and obtains the quality representation of the video, $\mathbf{z} \in \mathbb{R}^{128 \times 1}$, which is expected to represent the quality of this sequence. This is used to calculate the quality-aware loss. On the other hand, we perform average pooling on the processed frame embeddings in the last recurrent iteration, $[\tilde{\mathbf{h}}_{T-N+1} \circ \tilde{\mathbf{h}}_{T-N+2} \circ \dots \circ \tilde{\mathbf{h}}_T]$, to generate a content embedding, $\mathbf{h}^c \in \mathbb{R}^{2048 \times 1}$. We also feed the memory token generated in the second last recurrent iteration, $\mathbf{h}_{\text{mem}}^{S-1}$, into a prediction network [5], $f(\cdot)$, to obtain the predicted content embedding $\hat{\mathbf{h}}^c$. Both \mathbf{h}^c and $\hat{\mathbf{h}}^c$ are then passed to the same projector, $g(\cdot)$, to obtain their corresponding content representation, $\mathbf{c} \in \mathbb{R}^{128 \times 1}$, and the predicted content representation, $\hat{\mathbf{c}} \in \mathbb{R}^{128 \times 1}$, respectively, which are used to calculate the content-aware loss.

To enable contrastive learning, a batch ($2B$) of training patches are fed into the network with B randomly selected patches of size $256 \times 256 \times 3 \times 72$ and their corresponding down-sampled versions ($128 \times 128 \times 3 \times 72$). The latter is used here to provide true positive pairs (for the calculation of the quality-aware loss) in contrastive learning as in [37]. The contrastive loss function contains two components, quality-aware and content-aware losses.

Quality-aware loss focuses on distinguishing videos based on the similarity of their visual quality. For a given input patch, the positive pairs are constituted either between the patches with similar quality or between a full-resolution patch and its corresponding low-resolution counterpart. The quality-aware loss, L_i^{quality} , for the i^{th} input patch in a batch is defined by:

$$L_i^{\text{quality}} = -\frac{1}{P_i} \sum_{j=1}^{P_i} \log \left(\frac{\exp(\phi(\mathbf{z}_i, \mathbf{z}_j)/\tau)}{\sum_{k=1, k \neq i}^{2B} \exp(\phi(\mathbf{z}_i, \mathbf{z}_k)/\tau)} \right). \quad (5)$$

Here P_i represents the number of patches (positive pairs) in a batch with the same quality interval (the classification process is described below) as patch i , or with the similar content to patch i but in

different resolutions. ϕ stands for the normalised dot product function, $\phi(a, b) = a^T b / (\|a\|_2 \|b\|_2)$, which measures the similarity between a and b . τ is a temperature parameter that is less than 1.

Quality classification. To support quality-aware learning, we employ a proxy quality metric to perform quality classification, inspired by the ranking-based training methodology proposed in RankD-VQA [13]. Specifically, we first use VMAF [31] to calculate the quality index for each patch by comparing it with the associated corresponding reference (see subsection 3.2). During the training process, for patch i , if another patch j is associated with a VMAF value close to that of patch i (the difference is smaller than a threshold TH),

$$|\text{VMAF}_i - \text{VMAF}_j| \leq \text{TH}, \quad (6)$$

these are considered as a positive pair. Similarly as in [13], although VMAF [31] does not offer a perfect correlation performance with groundtruth subjective opinions, with a sensible threshold value, the classification here can be considered to be reliable (with a 95%+ accuracy), as demonstrated in [13]).

Content-aware loss captures the content dependent nature of video enhancement methods, providing a different observation aspect in the training process. This has been reported to be effective in the literature [5] for the video quality assessment task. In our case, the positive pair from the content perspective is defined for patches with the same source content.

Specifically, given the content representation \mathbf{c}_i and its predicted version $\hat{\mathbf{c}}_i$ for patch i in a batch, the content-aware loss is calculated by:

$$L_i^{\text{content}} = -\frac{1}{C_i} \sum_{j=1}^{C_i} \log \left(\frac{\exp(\phi(\mathbf{c}_i, \mathbf{c}_j)/\tau) + \exp(\phi(\mathbf{c}_i, \hat{\mathbf{c}}_j)/\tau)}{\sum_{k=1, k \neq i}^B (\exp(\phi(\mathbf{c}_i, \mathbf{c}_k)/\tau) + \exp(\phi(\mathbf{c}_i, \hat{\mathbf{c}}_k)/\tau))} \right), \quad (7)$$

where C_i represents the number of patches in a batch with the same content as patch i .

Similarly as in [22], the final contrastive loss is defined as a weighted sum of the quality- and content-aware components:

$$L = \frac{1}{B} \sum_{i=1}^B \left(L_i^{\text{quality}} + \lambda_1 L_i^{\text{content}} \right), \quad (8)$$

where λ_1 is a tuning parameter. Here we only consider full-resolution patches when calculating the final contrastive loss.

4 Experimental Configuration

Implementation Details. The implementation of the RMViT module is based on the Vision transformer for small dataset [28], where the depth is set to 8 and the number of heads is 64. The hidden dimension is adjusted to 2048 following the practice in [37]. The size of the segment is fixed at 4. The number of memory tokens and the segment length are 12 (this is verified in *Supplementary* through an analysis of the training results). The batch size for training is $B = 256$. τ is set to 0.1. The threshold TH, used in the quality classification, is set to 6 based on [13]. Data augmentation is performed during the training content generation through block rotation. The RMViT module, the prediction network, $f(\cdot)$, and the projector network, $g(\cdot)$, were trained simultaneously from scratch for 150 epochs using stochastic gradient descent (SGD) at a learning rate of 0.00025. A linear warmup over the first ten epochs was applied to the learning rate, followed by a cosine decay schedule used in [33]. The proposed method was implemented using Pytorch 1.13 with an NVIDIA 3090 GPU.

Evaluation settings. To demonstrate the effectiveness of the proposed RMT-BVQA, we compared it with two classic, two regression-based and six deep blind VQA methods. Due to the limited test content available, we performed a five-fold cross validation experiment based on the VDPVE database² for RMT-BVQA and all the other eight learning-based VQA methods. This dataset is further divided into three sub-datasets: Subset A including 414 videos generated through colour, brightness, and contrast enhancement; Subset B comprising 210 deshaked videos; and Subset C

²Here we refer to the VDPVE training set, which contains 839 sequences, while the test set is not accessible.

NR Metrics	Subset A		Subset B		Subset C		Overall	
	SRCC	PLCC	SRCC	PLCC	SRCC	PLCC	SRCC	PLCC
NIQE [41]	0.3555	0.4485	0.5830	0.6108	0.0540	0.2079	0.1401	0.2411
VIIDEO [40]	0.1468	0.3484	0.0854	0.3387	0.2701	0.3104	0.0646	0.2574
V-BLIINDS [46]	0.7214	0.7691	0.7028	0.7196	0.7055	0.7104	0.7106	0.7301
TLVQM [24]	0.6942	0.7085	0.5619	0.5940	0.5457	0.6001	0.5861	0.6499
BVQA [29]	0.5477	0.5596	0.3986	0.4271	0.3403	0.3872	0.4655	0.4807
VSFA [30]	0.4803	0.4912	0.5315	0.5696	0.6564	0.6911	0.5282	0.5473
ChipQA [11]	0.4572	0.4756	0.3347	0.3753	0.7713	0.7759	0.5639	0.5285
CONVIQT [38]	0.7411	0.7639	0.4174	0.6926	0.6678	0.7192	0.7052	0.7297
FAST-VQA [52]	0.7022	0.7147	0.7398	0.7706	0.8356	0.8677	0.7196	0.7644
RankDVQA-NR [13]	0.6620	0.6703	0.6623	0.6527	0.5524	0.4872	0.6197	0.5777
RMT-BVQA (ours)	0.8164	0.8139	0.8012	0.8019	0.8315	0.8385	0.8209	0.8384
v1-GRU	0.7906	0.8012	0.5585	0.6085	0.8128	0.8209	0.7852	0.7880
v2-quality	0.8019	0.8023	0.7989	0.8049	0.7864	0.8075	0.8052	0.8255

Table 2: Summary of the comparison and ablation study results. Here the best and second best results in each column are highlighted in red and blue colours, respectively.

containing 215 deblurred videos. It should be noted that for the proposed method, only the linear regression is optimised using the training set in the cross validation. The five-fold cross validation has been performed 100 times to calculate the average correlation coefficients. To test the correlation performance with subjective opinions, we employed both the SRCC and the Pearson Linear Correlation Coefficient (PLCC) as evaluation metrics. We have also compared our approach with the other ten VQA methods in terms of their computational complexity. However, due to limited space in the main paper, we include the complexity results in the *Supplementary*.

5 Experiments and Results

Table 2 summarises the comparison results between our proposed method, RMT-BVQA, and ten benchmark VQA methods³. It can be observed that RMT-BVQA offers the best overall performance among all the tested quality metrics - the only one with SRCC and PLCC values above 0.8. For all three subsets, A, B, and C in the VDPVE database, which correspond to different enhancement method types, our model is the best performer on Subset A and B, and the second best on Subset C (very close to FAST-VQA). Figure 2 provides three visual examples in which the proposed RMT-BVQA offers the correct quality differentiation as human perception, while the second best performer, FAST-VQA [52] fails to do that.

To further verify the effectiveness of the main contributions in this work, an ablation study is also conducted including the following sub tests.

Recurrent Memory Vision Transformer. We evaluated the contribution of our RMViT module by replacing it with an alternative network structure, Gates Recurrent Unit (GRU) [7], which has been utilised in previous contrastive learning based video quality assessment tasks [38]. The new variant is denoted by (v1-GRU).

Content-quality-aware contrastive learning. We further verify the effectiveness of the proposed content-quality-aware loss function by removing the content-aware loss, producing (v2-quality). We did not test the contribution of the quality-aware loss, because only employing content-aware loss leads to unstable training performance.

The training database. Since it is difficult to find an alternative to the proposed training database, which can support the optimisation of the RMViT module, we instead compared v1-GRU to the original CONVIQT model to verify the contribution of the training database. v1-GRU effectively

³It is noted that the results presented here are different from [32], where the test set (unavailable publicly) of the VDPVE database was employed for evaluation.

$\sqrt{60.83}$	Human	49.93	$\sqrt{51.42}$	Human	41.49	63.92	Human	80.93 $\sqrt{}$
0.499	FAST-VQA	0.512 $\sqrt{}$	0.374	FAST-VQA	0.398 $\sqrt{}$	$\sqrt{0.947}$	FAST-VQA	0.912
$\sqrt{66.58}$	RMT-BVQA	54.04	$\sqrt{49.62}$	RMT-BVQA	45.49	54.52	RMT-BVQA	57.74 $\sqrt{}$

Figure 2: Visual examples from three subsets of VDPVE [14] (from the left to the right: colour transform, deshaking and deblurring) demonstrating the superiority of the proposed method. In these three cases, RMT-BVQA (ours) provides the same quality differentiation as human perception does.

has the same network architecture as CONVIQT - differing only in the use of the new training database to optimise the GRU module.

The results of the ablation study are also provided in Table 1, where both v1-GRU and v2-quality achieve lower average correlation coefficients compared to RMT-BVQA. It can be observed that v1-GRU outperforms CONVIQT, with better overall correlation performance as shown in Table 2, confirming the effectiveness of the developed training database.

6 Conclusion

In this paper, we propose a blind deep VQA method specifically for enhanced video content based on a novel self-supervised learning training methodology. In this work, we designed a new Recurrent Memory Vision Transformer (RMViT) module to obtain video quality representations, which is optimised through contrastive learning based on a content-quality-aware loss function. A large and diverse training dataset has also been developed containing various types of enhanced video content. The proposed method, RMT-BVQA, has been tested on a video enhancement quality database through five-fold cross validation, and exhibits higher correlation with opinion scores when compared to ten existing no-reference VQA methods. Future work should focus on benchmarking on more diverse enhanced video content.

References

- [1] S. Ahn and S. Lee. Deep blind video quality assessment based on temporal human perception. In *2018 25th IEEE International Conference on Image Processing (ICIP)*, pages 619–623. IEEE, 2018.
- [2] A. Bulatov, Y. Kuratov, and M. Burtsev. Recurrent memory transformer. *Advances in Neural Information Processing Systems*, 35:11079–11091, 2022.
- [3] D. R. Bull and F. Zhang. *Intelligent image and video compression: communicating pictures*. Academic Press, 2021.
- [4] K. C. K. Chan, S. Zhou, X. Xu, and C. C. Loy. BasicVSR++: Improving video super-resolution with enhanced propagation and alignment. *2022 IEEE/CVF Conference on Computer Vision and Pattern Recognition (CVPR)*, pages 5962–5971, 2021.
- [5] P. Chen, L. Li, J. Wu, W. Dong, and G. Shi. Contrastive self-supervised pre-training for video quality assessment. *IEEE Transactions on Image Processing*, 31:458–471, 2022.
- [6] Z. Chen, Y. Zhang, D. Liu, J. Gu, L. Kong, X. Yuan, et al. Hierarchical integration diffusion model for realistic image deblurring. *Advances in Neural Information Processing Systems*, 36, 2024.
- [7] K. Cho, B. Van Merriënboer, D. Bahdanau, and Y. Bengio. On the properties of neural machine translation: Encoder-decoder approaches. *arXiv preprint arXiv:1409.1259*, 2014.
- [8] M. Coltheart. Iconic memory and visible persistence. *Perception & Psychophysics*, 27:183–228, 1980.
- [9] A. Danielyan, V. Katkovich, and K. Egiazarian. BM3D frames and variational image deblurring. *IEEE Transactions on image processing*, 21(4):1715–1728, 2011.
- [10] D. Danier, F. Zhang, and D. Bull. LDMVFI: Video frame interpolation with latent diffusion models. In *Proceedings of the AAAI Conference on Artificial Intelligence*, volume 38, pages 1472–1480, 2024.

- [11] J. P. Ebenezer, Z. Shang, Y. Wu, H. Wei, S. Sethuraman, and A. C. Bovik. ChipQA: No-reference video quality prediction via space-time chips. *IEEE Transactions on Image Processing*, 30:8059–8074, 2021.
- [12] C. Feng, D. Danier, C. Tan, F. Zhang, and D. Bull. ViSTRA3: Video coding with deep parameter adaptation and post processing. In *2022 IEEE International Symposium on Circuits and Systems (ISCAS)*, pages 824–828, 2022.
- [13] C. Feng, D. Danier, F. Zhang, and D. Bull. RankDVQA: Deep vqa based on ranking-inspired hybrid training. In *Proceedings of the IEEE/CVF Winter Conference on Applications of Computer Vision*, pages 1648–1658, 2024.
- [14] Y. Gao, Y. Cao, T. Kou, W. Sun, Y. Dong, X. Liu, X. Min, and G. Zhai. VDPVE: Vqa dataset for perceptual video enhancement. In *Proceedings of the IEEE/CVF Conference on Computer Vision and Pattern Recognition*, pages 1474–1483, 2023.
- [15] J. Geo, D. Jain, and A. Rajwade. GlobalFlowNet: Video stabilization using deep distilled global motion estimates. In *2023 IEEE/CVF Winter Conference on Applications of Computer Vision (WACV)*, pages 5067–5076, 2023.
- [16] P. Getreuer. Automatic color enhancement (ACE) and its fast implementation. *Image Process. Line*, 2:266–277, 2012.
- [17] D. Ghadiyaram, J. Pan, A. C. Bovik, A. K. Moorthy, P. Panda, and K.-C. Yang. In-capture mobile video distortions: A study of subjective behavior and objective algorithms. *IEEE Transactions on Circuits and Systems for Video Technology*, 28(9):2061–2077, 2018.
- [18] K. He, X. Zhang, S. Ren, and J. Sun. Deep residual learning for image recognition. In *Proceedings of the IEEE Conference on Computer Vision and Pattern Recognition*, pages 770–778, 2016.
- [19] V. Hosu, F. Hahn, M. Jenadeleh, H. Lin, H. Men, T. Szirányi, S. Li, and D. Saupe. The Konstanz natural video database (KoNViD-1k). In *2017 Ninth International Conference on Quality of Multimedia Experience (QoMEX)*, pages 1–6, 2017.
- [20] D.-J. Huang, Y.-T. Kao, T.-H. Chuang, Y.-C. Tsai, J.-K. Lou, and S.-H. Guan. SB-VQA: A stack-based video quality assessment framework for video enhancement. In *Proceedings of the IEEE/CVF Conference on Computer Vision and Pattern Recognition*, pages 1613–1622, 2023.
- [21] A. Jaiswal, A. R. Babu, M. Z. Zadeh, D. Banerjee, and F. Makedon. A survey on contrastive self-supervised learning. *Technologies*, 9(1):2, 2020.
- [22] P. Khosla, P. Teterwak, C. Wang, A. Sarna, Y. Tian, P. Isola, A. Maschinot, C. Liu, and D. Krishnan. Supervised contrastive learning. *Advances in Neural Information Processing Systems*, 33:18661–18673, 2020.
- [23] J. Kim and S. Lee. Deep learning of human visual sensitivity in image quality assessment framework. In *2017 IEEE Conference on Computer Vision and Pattern Recognition (CVPR)*, pages 1969–1977, 2017.
- [24] J. Korhonen. Two-level approach for no-reference consumer video quality assessment. *IEEE Trans. on Image Processing*, 28(12):5923–5938, 2019.
- [25] O. Kupyn, T. Martyniuk, J. Wu, and Z. Wang. DeblurGAN-v2: Deblurring (orders-of-magnitude) faster and better. In *2019 IEEE/CVF International Conference on Computer Vision (ICCV)*, pages 8877–8886, 2019.
- [26] K. Lamichhane, P. Mazumdar, F. Battisti, and M. Carli. A no reference deep learning based model for quality assessment of ugc videos. In *2021 IEEE International Conference on Multimedia & Expo Workshops (ICMEW)*, pages 1–5, 2021.
- [27] P. H. Le-Khac, G. Healy, and A. F. Smeaton. Contrastive representation learning: A framework and review. *Ieee Access*, 8:193907–193934, 2020.
- [28] S. H. Lee, S. Lee, and B. C. Song. Vision transformer for small-size datasets. *arXiv preprint arXiv:2112.13492*, 2021.
- [29] B. Li, W. Zhang, M. Tian, G. Zhai, and X. Wang. Blindly assess quality of in-the-wild videos via quality-aware pre-training and motion perception. *IEEE Transactions on Circuits and Systems for Video Technology*, 32(9):5944–5958, 2022.
- [30] D. Li, T. Jiang, and M. Jiang. Quality assessment of in-the-wild videos. In *Proceedings of the 27th ACM International Conference on Multimedia*, pages 2351–2359, 2019.
- [31] Z. Li, A. Aaron, I. Katsavounidis, A. Moorthy, and M. Manohara. Toward a practical perceptual video quality metric. *The Netflix Tech Blog*, 2016.
- [32] X. Liu, R. Timofte, Y. Dong, Z. Ma, H. Fan, C. Zhu, X. Min, G. Zhai, Z. Jia, M. Agarla, et al. NTIRE 2023 quality assessment of video enhancement challenge. In *Proceedings of the IEEE/CVF Conference on Computer Vision and Pattern Recognition*, pages 1551–1569, 2023.

- [33] I. Loshchilov and F. Hutter. SGDR: Stochastic gradient descent with warm restarts. In *International Conference on Learning Representations*, 2017.
- [34] F. Lv, F. Lu, J. Wu, and C. S. Lim. MBLEN: Low-light image/video enhancement using CNNs. In *British Machine Vision Conference*, 2018.
- [35] D. Ma, F. Zhang, and D. R. Bull. BVI-DVC: A training database for deep video compression. *IEEE Transactions on Multimedia*, 24:3847–3858, 2022.
- [36] D. Ma, F. Zhang, and D. R. Bull. CVEGAN: a perceptually-inspired GAN for compressed video enhancement. *Signal Processing: Image Communication*, page 117127, 2024.
- [37] P. C. Madhusudana, N. Birkbeck, Y. Wang, B. Adsumilli, and A. C. Bovik. Image quality assessment using contrastive learning. *IEEE Transactions on Image Processing*, 31:4149–4161, 2022.
- [38] P. C. Madhusudana, N. Birkbeck, Y. Wang, B. Adsumilli, and A. C. Bovik. CONVIQT: Contrastive video quality estimator. *IEEE Transactions on Image Processing*, 32:5138–5152, 2023.
- [39] A. Mittal, A. K. Moorthy, and A. C. Bovik. No-reference image quality assessment in the spatial domain. *IEEE Transactions on Image Processing*, 21(12):4695–4708, 2012.
- [40] A. Mittal, M. A. Saad, and A. C. Bovik. A completely blind video integrity oracle. *IEEE Trans. on Image Processing*, 25(1):289–300, 2015.
- [41] A. Mittal, R. Soundararajan, and A. C. Bovik. Making a “completely blind” image quality analyzer. *IEEE Signal Processing Letters*, 20(3):209–212, 2012.
- [42] P. Ndjiki-Nya, D. Doshkov, H. Kaprykowsky, F. Zhang, D. Bull, and T. Wiegand. Perception-oriented video coding based on image analysis and completion: A review. *Signal Processing: Image Communication*, 27(6):579–594, 2012.
- [43] Ofcom. Media nations uk 2023, 2023.
- [44] A. P. Pro.
- [45] Z. Qi, C. Feng, D. Danier, F. Zhang, X. Xu, S. Liu, and D. Bull. Full-reference video quality assessment for user generated content transcoding. *arXiv preprint arXiv:2312.12317*, 2023.
- [46] M. A. Saad, A. C. Bovik, and C. Charrier. Blind prediction of natural video quality. *IEEE Transactions on Image Processing*, 23(3):1352–1365, 2014.
- [47] M. Shahid, A. Rossholm, B. Lövsström, and H.-J. Zepernick. No-reference image and video quality assessment: a classification and review of recent approaches. *EURASIP Journal on Image and Video Processing*, 2014:1–32, 2014.
- [48] Z. Sinno and A. C. Bovik. Large-scale study of perceptual video quality. *IEEE Transactions on Image Processing*, 28(2):612–627, 2018.
- [49] TikTok. Capcut pro.
- [50] Z. Tu, Y. Wang, N. Birkbeck, B. Adsumilli, and A. C. Bovik. UGC-VQA: Benchmarking blind video quality assessment for user generated content. *IEEE Trans. on Image Processing*, 30:4449–4464, 2021.
- [51] Y. Wang, S. Inguva, and B. Adsumilli. YouTube UGC dataset for video compression research. In *2019 IEEE 21st International Workshop on Multimedia Signal Processing (MMSP)*, pages 1–5, 2019.
- [52] H. Wu, C. Chen, J. Hou, L. Liao, A. Wang, W. Sun, Q. Yan, and W. Lin. FAST-VQA: Efficient end-to-end video quality assessment with fragment sampling. In *European Conference on Computer Vision*, pages 538–554, 2022.
- [53] W. Wu, S. Hu, P. Xiao, S. Deng, Y. Li, Y. Chen, and K. Li. Video quality assessment based on swin transformer with spatio-temporal feature fusion and data augmentation. In *Proceedings of the IEEE/CVF Conference on Computer Vision and Pattern Recognition*, pages 1846–1854, 2023.
- [54] J. Xu, P. Ye, Y. Liu, and D. Doermann. No-reference video quality assessment via feature learning. In *2014 IEEE International Conference on Image Processing (ICIP)*, pages 491–495. IEEE, 2014.
- [55] M. Xu, J. Chen, H. Wang, S. Liu, G. Li, and Z. Bai. C3DVQA: Full-reference video quality assessment with 3D convolutional neural network. In *ICASSP 2020 - 2020 IEEE International Conference on Acoustics, Speech and Signal Processing (ICASSP)*, pages 4447–4451, 2020.
- [56] F. Zhang, M. Afonso, and D. R. Bull. ViSTRA2: Video coding using spatial resolution and effective bit depth adaptation. *Signal Processing: Image Communication*, 97:116355, 2021.
- [57] F. Zhang, D. Ma, C. Feng, and D. R. Bull. Video compression with CNN-based postprocessing. *IEEE MultiMedia*, 28(4):74–83, 2021.
- [58] Z. Zhang, H. Zheng, R. Hong, M. Xu, S. Yan, and M. Wang. Deep color consistent network for low-light image enhancement. In *Proceedings of the IEEE/CVF Conference on Computer Vision and Pattern Recognition*, pages 1899–1908, 2022.

- [59] K. Zhao, K. Yuan, M. Sun, M. Li, and X. Wen. Quality-aware pre-trained models for blind image quality assessment. In *Proceedings of the IEEE/CVF Conference on Computer Vision and Pattern Recognition*, pages 22302–22313, 2023.
- [60] Z. Zhong, Y. Gao, Y. Zheng, and B. Zheng. Efficient spatio-temporal recurrent neural network for video deblurring. In *European Conference on Computer Vision*, pages 191–207, 2020.